INFORMATION TO USERS

This manuscript has been reproduced from the microfilm master. UMI films the text directly from the original or copy submitted. Thus, some thesis and dissertation copies are in typewriter face, while others may be from any type of computer printer.

The quality of this reproduction is dependent upon the quality of the copy submitted. Broken or indistinct print, colored or poor quality illustrations and photographs, print bleedthrough, substandard margins, and improper alignment can adversely affect reproduction.

In the unlikely event that the author did not send UMI a complete manuscript and there are missing pages, these will be noted. Also, if unauthorized copyright material had to be removed, a note will indicate the deletion.

Oversize materials (e.g., maps, drawings, charts) are reproduced by sectioning the original, beginning at the upper left-hand corner and continuing from left to right in equal sections with small overlaps.

ProQuest Information and Learning
300 North Zeeb Road, Ann Arbor, MI 48106-1346 USA
800-521-0600

UNIVERSITY OF CINCINNATI

May 22 19 53

I hereby recommend that the thesis prepared under my supervision by David F. Edwards

entitled NUCLEAR SHELL MODEL TO ACCOUNT FOR BINDING ENERGY DISCONTINUITIES

be accepted as fulfilling this part of the requirements for the degree of DOCTOR OF PHILOSOPHY

Approved by:

Alex E. S. Green

Boris Podolsky

Harold J. Kerstein

Form 668—G.S. and T.C.—1M—4-51

NUCLEAR SHELL MODEL TO ACCOUNT FOR BINDING ENERGY DISCONTINUITIES

A dissertation submitted to the
Graduate School of Arts and Sciences of the
University of Cincinnati

in partial fulfillment of the
requirements for the degree of

DOCTOR OF PHILOSOPHY

1953

by

David F. Edwards

A.B. Miami University 1949

M.S. University of Cincinnati 1951

Table of Contents

Introduction

This paper is an investigation of the discontinuities of the neutron and proton binding energies associated with the closing and opening of nuclear shells. These binding energies are analyzed in such a way as to give estimates of the effects associated with the pairing tendency of nuclei and the shell structure. The analysis of the data and consideration of an atomic model lead to a simple approximate representation of a shell stabilizing correction to the nuclear energies. Similiarities of the binding energy diagrams of the last nucleons and the last electron are noted. Insight into nuclear shell structure would be possible from a theory that will describe the saw-toothed curve of the atomic ionization potentials. Because of the enormous amount of work that has been done in the prediction of x-ray levels of the atom, this was considered a relatively simple problem and of just a secondary nature. However, a search of the literature for such a quantum mechanical theory has been unfruitful. It seems that for some reason this problem has been avoided. This problem is investigated here (see final sections of this paper) under the assumption that the electrons have the nature of the Fermi-Thomas gas. An approximate expression is given by which the ionization potentials for each element in the periodic system ($Z>10$) might be calculated.

Chapters 2 - 8 of this paper, exclusive of some of the intermediate steps, are to be published in the Physical Review, July 1, 1953 as a joint work with Alex E. S. Green. These chapters were also presented at the 1953 Washington Meeting of the American Physical Society by Alex E. S. Green and this author, Bull. Am. Phys. Soc. 28, No. 3, 19.

1. The Empirical Mass Surface.

The solution of many atomic problems have been possible from our knowledge of the charge of the nucleus. With the exception of the very small corrections, e.g. hyperfine structure, isotope shift of spectral lines, etc., all the properties of the atom can be described from this knowledge. The detailed nature of the electron-nuclear interaction was accurately known from electrostatic interaction experiments. This long range coulomb interaction was found to be the dominant effect. The atomic model became that of light negatively charged particles, the electrons, moving somewhat independently about a massive positively charged nucleus with this coulombic interaction. Since the principle force of interaction was known, the problem of the atomic physicists was to find the proper mechanics which would describe the motion of the particles with a given force. The result, as we know, was the introduction of quantum mechanics.

The solution of the nuclear problem is quite different. Here the field theory which would give the nature of the interaction between nucleons, i.e. protons and neutrons, is not completely known. The nucleus cannot be pictured as a system of particles moving about a massive center. From the study of α-disintegrations it is suggested that quantum mechanics might also describe the motion of nucleons. Several nuclear phenomena have been successfully described by the independent-particle model. The independent-particle model was first introduced into atomic physics by Hartree [1] and has been used there with great success. A good discussion of this model for the nucleus is given by J. W. Blatt and V. F. Weisskopf, Theoretical Nuclear Physics,

Wiley (1952). The independent particle model assumes that each nucleon moves independently of all other nucleons in a common potential field. This field represents the average effect of all the interactions with the other nucleons. In general, however, the field theoretical approach has been unsuccessful. Another attempt to predict the nuclear phenomena is by a phenomenological approach. That is, by assuming some statistical model of the nucleus, inferring an interaction function to correlate all the experimental information concerning the interaction in terms of certain arbitrary constants. These constants are then adjusted to the experimental data and hence the name phenomenological. An early model of this type that has proved to be the prototype of several successful ones is that due to Weizsäcker.[2]

The test of either approach to the solution of the nuclear interaction, field theoretical or phenomenological, is the ability to predict additional information which is consistent with experiment.

The phenomenological approach to nuclear problems is the concern of this thesis. A method introduced by Alex E. S. Green[3] is used here as a tool in the analysis of the data. The approach is to express the mass or energy parameters in terms of the mass decrement or sometimes called the mass defect, Δ . The mass decrement is defined as the difference between the actual atomic mass, M , and the integral mass number, A , ($\Delta = M - A$). Δ is conveniently expressed in milli-mass units (mMU). The mass decrement gives direct information about the binding energies of the particles in a nucleus.

The mass decrement which is usually regarded as a function of A and D ($= N - Z$, the neutron excess) can also be expressed as a function

of the neutron and proton numbers N and Z, respectively. This follows from the definition of the neutron excess, D (sometimes referred to as the isotopic number, I).

It has become accepted in the literature to consider this function, $\Delta(A,D)$, as a three dimensional surface. The surface is shaped like a valley or trench and is referred to as the "mass surface". Green's mass decrement surface[4] is given as:

$$\Delta(A,D) = \Delta_m(A) + \delta H(A) + \Theta^2 J(A)$$

$$= 100(\tilde{A}-1)^2 - 64 + \delta/\tilde{A}^{1/2} + \Theta^2/4\tilde{A} \quad , \qquad (1.1)$$

where by definition $\tilde{A} = A/100$, $\Theta = N - Z - D_m = D - D_m = D - 40\tilde{A}^2/(\tilde{A}+2)$, and $\delta = -1, 0$ or $+1$ for OO, EO or OE and EE type nuclides[5] respectively. This representation has the advantage that the EE, OO and EO-OE surfaces are themselves relatively smooth surfaces. The function $D_m(A)$ locates the minimum of the valley and $\Delta_m(A)$ the depth. The parabolic isobaric sections are characterized by the functions Θ $(= D - D_m(A))$ and $J(A)$. The additional energy due to the pairing tendencies of the nucleons is given by $\delta/\tilde{A}^{1/2}$.

In a recent paper by Green and Engler,[6] it has been pointed out that for many purposes it is sufficient to represent the nuclear mass decrements by a smooth function of mass number alone. They give this as

$$\Delta^r_m(A) = (A-100)^2/100 - 64 \quad . \qquad (1.2)$$

Throughout this work $\Delta^r_m(A)$ is used as a reference function.

2. The Data and Their Interpretation.

In the first part of this paper an investigation of the neutron and proton binding energies is made in such a way as to permit an approximate assessment of the effects associated with pairing and shell structure. These effects are inferred from the local deviations of the mass surface from the smooth function Eq. (1.2). To facilitate the analysis of the discontinuities in the experimental mass surface, it has been advantageous to convert the experimental data into a set of mass residuals and reaction energy or Q-value residuals. The mass residual, in mMU , for a particular nuclide is here defined as

$$R = \Delta - \Delta^{r}_{m}(A) \quad , \qquad (2.1)$$

where Δ is the experimental mass decrement and Δ^{r}_{m} is given by Eq. (1.2). The Q-value residual is defined (GE Eq. (20)) as:

$$R(Q) = Q - Q^{r}_{m}(A) \quad . \qquad (2.2)$$

By referring the mass decrements and Q-values to $\Delta^{r}_{m}(A)$ and $Q^{r}_{m}(A)$ instead of the complete reference functions (GE Eqs. 1 and 16), the task of computing residuals is greatly simplified. At the same time there are still the advantages of reference functions which are good approximations to the actual functions.

For studying shell and pairing discontinuities in the nuclear mass surface, the mass residuals are assumed to be represented by

$$R(N,Z) = S_{ij}(N,Z) + P(N,Z) + J^{o}\left[D - D^{o}_{m}(A)\right]^{2} \quad . \qquad (2.3)$$

The subscript i is used to denote a region of the mass surface lying between the planes defined by the magic neutron numbers N_u and N_l and the subscript j is used to denote a region lying between planes defined by the magic proton numbers Z_u and Z_l, (See Table II or Fig. 6).

$S_{ij}(N,Z)$ is assumed to embody the shell structure effect and $P(N,Z)$ is now used to represent the pairing effect. It will be assumed that

$$P(O,O) = H, \qquad P(E,E) = -H,$$
$$P(E,O) = p, \qquad P(O,E) = n, \qquad (2.4)$$

where E and O denote the evenness or oddness of N or Z respectively. Thus the convention of referring masses to a surface which lies half way between the even-even and odd-odd nuclear surfaces is retained for this discussion. There is allowance now, however, for the possible departures of the two odd mass surfaces from this intermediate surface. The parabolic term contains the optimum smooth functions for the line of stability and the parabolic width (GE Eqs. 10 and 11, respectively).

When both the target and product nuclides belong to the same zone, the Q-value residual is

$$R(Q) = S_{ij}(N,Z) - S_{ij}(N',Z') + P(N,Z) - P(N',Z') + J^0\theta^2 - J'^0\theta'^2, \qquad (2.5)$$

where $\theta = D - D^0_m(A)$ and $\theta' = D' - D^0_m(A)$. Since the changes in N, Z and A are usually small compared to N, Z, and A, this equation can be expressed approximately as

$$R(Q) \cong (n-n')\frac{\partial S_{ij}}{\partial N} + (z-z')\frac{\partial S_{ij}}{\partial Z} + p - p' + J^0(\theta^2 - \theta'^2), \qquad (2.6)$$

where n, n', z and z' are the neutron and proton numbers of the incident

and ejected particles. Thus, apart from the spin and parabolic effect, residual Q-values are related to the partial derivatives of the shell function. The problem of apportioning the residual Q-values to the four terms on the right side of Eq. (2.6) is complicated by the fact that these terms are frequently of the same order of magnitude. Fortunately by the judicious choice of data for study, the problem becomes tractable.

3. Neutron and Proton Binding Energies.

Neutron and proton binding energies furnish a good source of data for studying shell effects since in these cases either the first or second term in Eq. (2.6) vanishes. Neutron and proton binding energies are defined as

$$B_N(N,Z) = M(N-1,Z) + m_N - M(N,Z) \quad , \tag{3.1}$$

and

$$B_P(N,Z) = M(N,Z-1) + m_H - M(N,Z) \quad . \tag{3.2}$$

Remembering that $\Delta(N,Z) = M(N,Z) - A$, these can be written as

$$B_N(N,Z) = \Delta(N-1,Z) + \Delta_N - \Delta(N,Z) = -Q\left[X(n,\gamma)X'\right] , \tag{3.3}$$

and

$$B_P(N,Z) = \Delta(N,Z-1) + \Delta_H - \Delta(N,Z) = -Q\left[X(p,\gamma)X'\right] . \tag{3.4}$$

Subtracting Q_m^r from both sides of Eq. (3.3), one obtains the residual neutron binding energy

$$R_N(N,Z) = B_N(N,Z) - B_N^r(A) \quad . \tag{3.5}$$

$B_N^r(A)$ is just the negative of the $Q_m^r(A)$ for the (γ,n) reaction.

$$B_N^r(N) = -Q_m^r(A) = \Delta^r(N-1,Z) + \Delta_N - \Delta^r(N,Z) \quad , \qquad (3.6)$$

and a similiar expression for $B_p^r(A)$. Subtracting Eq. (3.6) from Eq. (3.3), then

$$B_N(N,Z) - B_N^r(A) = \Delta(N-1,Z) - \Delta_m^r(N-1,Z) - \{\Delta(N,Z) - \Delta_m^r(N,Z)\}$$
$$= R(N-1,Z) - R(N,Z) \quad . \qquad (3.7)$$

It follows then that

$$R_N(N,Z) = R(N-1,Z) - R(N,Z) \quad . \qquad (3.8)$$

Similiarly, for the residual proton binding energy,

$$R_p(N,Z) = B_p(N,Z) - B_p^r(A)$$
$$= R(N,Z-1) - R(N,Z) \quad . \qquad (3.9)$$

$B_N^r(A)$ and $B_p^r(A)$ are the reference functions found in Table III GE.

An extensive collection of neutron binding energies from (γ, n) thresholds, from the Q-values of (n,γ) reactions, and (d,p) reactions, and from mass data is available.[7] However, few proton binding energies have been measured directly. The residual proton binding energies may be computed from (p,n) reactions, (d,n) reactions and mass residual data. This can be seen by considering the difference

$$R_p(N,Z) - R_N(N,Z) = \{R(N,Z-1) - R(N,Z)\} - \{R(N-1,Z) - R(N,Z)\} \quad , (3.10)$$

which follows from (3.8) and (3.9). This simplifies to

$$R_p(N,Z) = R_N(N,Z) + [R(N,Z-1) - R(N-1,Z)] \quad . \qquad (3.11)$$

Since the difference between the mass residuals indicated in brackets is the same as the difference between masses,[8] this term may frequently be obtained from beta decay energies.

In view of Eqs. (3.3) and (3.4), as special cases of Eq. (2.6)

$$R_N(N,Z) = -\frac{\partial S_{ij}}{\partial N} + P' - P + J^\circ(\Theta'^2 - \Theta^2) \quad , \qquad (3.12)$$

and

$$R_P(N,Z) = -\frac{\partial S_{ij}}{\partial Z} + P' - P + J^\circ(\Theta'^2 - \Theta^2) \quad . \qquad (3.13)$$

The parabolic term presents considerable difficulties. Not only is it a tedious term to compute but it is particularly sensitive to a small fluctuation in the location of the valley. Since the shell effect is probably the main cause of fluctuations in the line of stability, the situation exists of having to know the shell correction in order to evaluate the shell correction. Fortunately, a successive approximation approach helps to resolve the difficulty. The approach which is adopted here is based upon an attempt to minimize the parabolic term by selecting pairs of nuclides which have at least one β-stable member. Since the change in Θ associated with the removal of a neutron or proton is of the order of +1 or -1 respectively, the difference of the squares may be expected to be a positive or negative number of the order of unity. Consequently, the parabolic correction term, as given by Green,[3] is of the order of $25/A$ which is relatively small for medium and heavy nuclides although appreciable for light nuclides. Accordingly, there must be expected scattering, particularly for small A, of the points from any smooth curve which represents the shell and spin corrections.

It has been pointed out that the pairing correction represents the additional energy due to unpaired nucleons. If the reference surface is taken as the EE surface, the additional energies of an EO, OE or OO nuclide may be denoted as π , ν and τ , respectively. These are the same π and ν as used by Coryell and Suess .[9] To allow for the possible interaction of the odd proton and odd neutron, the τ is not restricted to be equal to $\pi+\nu$. In Table I is shown an analysis of the pairing correction for the binding energies of protons and neutrons as they depend upon the nuclear type as given in column one. In columns 2 and 5 is indicated the pairing energy differences involved in these cases under the general assumption that the pairing energies take on the values $0, \pi, \nu$ and τ. In columns 3 and 6 is indicated what these differences would be if $\tau=\pi+\nu$. In columns 4 and 7 is indicated what these differences would be if $\pi=\nu=\tau/2=H$.

Ignoring momentarily the parabolic and pairing corrections, the neutron and proton binding energy residuals (Eqs. (3.12) and (3.13)) are just the negatives of the partial derivatives of the shell structure term. On plots of R_N vs N and R_P vs Z , the points corresponding to the nuclides should collect about the curves $-\frac{\partial S_{ij}}{\partial N}$ and $-\frac{\partial S_{ij}}{\partial Z}$ respectively. Taking into account the pairing term of Eqs. (3.12) and (3.13), one would expect, if $\tau=\pi+\nu$, that the experimental points will be above or below $-\frac{\partial S_{ij}}{\partial N}$ and $-\frac{\partial S_{ij}}{\partial Z}$ by the distances given in columns 3 and 6 of Table I. Accordingly the points on the R_N vs N plot should group in such a way that the curve $-\frac{\partial S_{ij}}{\partial N}$ would be half way between the average distributions of the EE, EO group and the OO, OE group. Similiarly for the R_P vs Z plot, the average distribution curves for

the EE, OE group and the OO, EO group should be equally spaced about the $-\frac{\partial S_{n,p}}{\partial Z}$ curve. One must expect random scattering about these distribution curves because of the parabolic factor. The distance between these average distribution curves on the R_n and R_p plots is expected to be 2ν and 2π, respectively. On the other hand, if τ differs from $\pi+\nu$, one would in both cases find four curves spaced with respect to $-\frac{\partial S_{n,p}}{\partial N}$ and $-\frac{\partial S_{n,p}}{\partial Z}$ in accordance with the columns 2 and 5 of Table I.

The neutron and proton binding energy residuals computed from recent experimental data[7] are shown in Figs. 1 and 2, respectively. To accommodate the computed residuals different vertical scales were used in Figs. 1 and 2.

4. The Pairing Effect.

By an examination of Figs. 1 and 2 one observes that to a large extent the grouping of types expected on the basis of the assumption that $\tau = \pi + \nu$ is fulfilled. In several instances significant departures seem to occur. The most noteworthy is in the region of A values between 230 and 240 where $\tau - (\pi+\nu) \cong 1$ (mMU).

In Fig. 3 is plotted the pairing energies, experimental and empirical, as functions of the mass number. The corresponding and numbers computed from the reference line of beta stability $\left\{ N^{\tau}_{m}(A) = \frac{1}{2}[A + D^{\tau}_{m}(A)] \right.$, $\left. Z^{\tau}_{m}(A) = \frac{1}{2}[A - D^{\tau}_{m}(A)] \right\}$ are also shown. The open circles and the closed circles represent estimated values of π and ν, respectively, for five unit intervals of N and Z. These values have been obtained from an analysis of the separation of the types in Fig. 1 and Fig. 2.

In Eq. (2.4) the surface which lies halfway between the EE and OO surfaces is taken as a reference. For the case $\pi \neq \nu$ it is permissible to let $H = \frac{1}{2}(\pi + \nu)$. Various functions of A have been proposed for this pairing correction. In Fig. 3 three of these functions are shown, $H_1(A) = 140/A$,[10] $H_2(A) = 36/A^{3/4}$,[11] and $H_3(A) = 10/A^{1/2}$.[3] Of these three, the last appears to best follow the variation with A . The function $12/A^{1/2}$ is probably still better although it is somewhat smaller in the middle range than the experimental data indicate.

Mayer ,[12] on the assumption of a delta function attractive potential for the spin orbit coupling model, obtains formulas for the pairing energy which may be expressed as

$$\pi = -c(j_\pi + \tfrac{1}{2})/A \qquad (4.1)$$

and

$$\nu = -c(j_\nu + \tfrac{1}{2})/A \quad , \qquad (4.2)$$

where j_π and j_ν is the total angular momentum of each proton or neutron in a given sub-shell and $c \cong 25$ Mev. . These values of π and ν are also plotted in Fig. 3. π is represented by the dashed lines and ν by the dash-dot lines. The j values are based on the spin orbit model as represented by the specific level scheme of Klinkenberg .[13] Only the average A are used for a particular sub-shell since according to Eqs. (4.1) and (4.2) the variation in π or ν within a sub-shell is small. For the moment one cannot say that Eqs. (4.1) and (4.2) are consistent with the experimental estimates of π and ν . The fact that Eqs. (4.1) and (4.2) are not inconsistent with the experimental values suggests that one must ultimately abandon efforts to represent the pairing effect

by the simple functions of mass number which are in common use.

The values of $\pi - \nu$ as found from the circles shown in Fig. 3 are in agreement, on the whole, with the values given by Coryell.[14]

5. A Reference Shell Correction.

From the scattering of the points in Figs. 1 and 2, it is obvious that a variety of $-\frac{\partial S_{ij}}{\partial N}$ and $-\frac{\partial S_{ij}}{\partial Z}$ curves may be chosen. To proceed further in an attempt to find a suitable representation of shell effects, it has been elected to represent these curves by the series of straight line segments. This representation is not only suggested by the proton and neutron binding energy data but it is also suggested by the irregularities in the corresponding ionization energy data in the atomic case.[15] More will be said about this atomic case in Chapters 9 and 11. Accordingly, for the nuclear shells, it is assumed that between any two major magic numbers the following relations exist:

$$-\frac{\partial S_{ij}}{\partial N} = 2\alpha_i (N - \tilde{N}_i) \qquad (5.1)$$

and

$$-\frac{\partial S_{ij}}{\partial Z} = 2\alpha_j (Z - \tilde{Z}_j) \quad , \qquad (5.2)$$

where α_i and α_j are proportional to the slopes of these straight line segments and $\tilde{N}_i$ and $\tilde{Z}_j$ are constants which must be adjusted for each region. In effect, it has been chosen to represent the shell correction by the series of functions

$$S_{ij}(N,Z) = -\alpha_i (N - \tilde{N}_i)^2 - \alpha_j (Z - \tilde{Z}_j)^2 + k_{ij} \quad . \qquad (5.3)$$

The shell function thus has the shape of an inverted cup with the peak value at $\tilde{N}_i$ and $\tilde{Z}_j$ points which usually lie intermediate between the boundaries of the zone. In Table II are listed the values of α_i, $\tilde{N}_i$, α_j and $\tilde{Z}_j$ obtained from a visual adjustment of the straight line segments in Figs. 1 and 2.

Consider now the manner in which the addition of a shell term given by Eq. (5.3) alters a mass decrement surface which has the basic form:

$$\Delta(A,D) = \Delta_m(A) + J\left[D - D_m(A)\right]^2 \quad . \tag{5.4}$$

Since the semi-empirical equation may be placed in this form the discussion is applicable to these equations as well as to the reference equation. Letting

$$N = \tfrac{1}{2}(A + D_m + D - D_m) = N_m(A) + \tfrac{1}{2}(D - D_m) \quad , \tag{5.5}$$

and

$$Z = \tfrac{1}{2}(A - D_m - D + D_m) = Z_m(A) - \tfrac{1}{2}(D - D_m) \quad , \tag{5.6}$$

and inserting these into the sum of Eq. (5.3) and Eq. (5.4), one finds it possible to express the result in each zone in the form of Eq. (5.4) if one lets

$$\Delta_m^{ij}(A) = \Delta_m(A) - \alpha_i\left[N_m(A) - \tilde{N}_i\right]^2 - \alpha_j\left[Z_m(A) - \tilde{Z}_j\right]^2 + te_{ij} - \frac{1}{4J^{ij}(A)}\left\{\alpha_i\left[N_m(A) - \tilde{N}_i\right] - \alpha_j\left[Z_m(A) - \tilde{Z}_j\right]\right\}^2 \quad , \tag{5.7}$$

$$D_m^{ij}(A) = D_m(A) + \left[\alpha_i(N_m - \tilde{N}_i) - \alpha_j(Z_m - \tilde{Z}_j)\right] / 2J^{ij}(A) \quad , \tag{5.8}$$

and

$$J^{ij}(A) = J(A) - (\alpha_i + \alpha_j)/4 \quad . \tag{5.9}$$

Rather than go further with the extensive set of empirical constants listed in Table II, one can without introducing considerable error replace these constants by the slightly different set:

$$\bar{\alpha}_i = (N_u - N_l)^{-1} \quad mMu \;, \quad \bar{\alpha}_j = (Z_u - Z_l)^{-1} \quad mMu \;, \tag{5.10}$$

$$\bar{N}_i = (N_u + N_l)/2 \quad , \quad \bar{Z}_j = (Z_u + Z_l)/2 \quad ,$$

where the subscripts u and l refer to the upper and lower magic numbers of the particular zone. In using these simple expressions for the parameters in the shell correction, the latitude now available has been exploited in view of the scattered data. Essentially the shell structure function is represented by the expression:

$$S_{ij}(N,Z) = -\frac{1}{N_u - N_l}\left(N - \frac{N_u + N_l}{2}\right)^2 - \frac{1}{Z_u - Z_l}\left(Z - \frac{Z_u + Z_l}{2}\right)^2 + k_{ij} \tag{5.11}$$

This expression, which of course must be treated only as a first approximation, has the distinct advantage of requiring only one empirical constant for each zone other than the magic numbers themselves. Using the smooth reference functions, the extent to which this reference shell function may account for effects attributed to shell structure are now investigated. Since the reference functions are "averages" of the semi-empirical functions much of this discussion pertains to these latter functions also.

6. The Shell Correction and the Line of Beta Stability.

In the paper by Green and Engler (See Fig. 3, GE), marked irregularities were noted in the function Υ which characterizes the deviations of the true line of stability from the reference function $D_m^r(A)$. To arrive at a more precise curve for Υ the results are presented here of an analysis based upon beta decay energies and mass data rather than stability limits. Let $D_m^{ij}(A)$ denote the true minimum of an isobaric section at mass number A. If the π, ν difference is ignored the mass difference between adjacent odd mass isobaric nuclides is

$$M^* - M_s = J^{ij}(A)\left\{\left[D^* - D_m^{ij}(A)\right]^2 - \left[D_s - D_m^{ij}(A)\right]^2\right\} , \qquad (6.1)$$

where the asterisk denotes a radionuclide and the subscript s the stable nuclide. Since $D^* = D_s \pm 2$, this becomes

$$M^* - M = 4J^{ij}(A)\left\{1 \pm \left[D - D_m^{ij}(A)\right]\right\} = r^{ij}\left[1 \pm (\theta - \Upsilon)\right]^{100/A} , \qquad (6.2)$$

where here

$$\theta = D - D_m^r(A) \qquad (6.3)$$

and

$$\Upsilon = D_m^{ij}(A) - D_m^r(A) \quad . \qquad (6.4)$$

If two mass differences are known, one may set up two equations and solve Eq. (6.2) for r^{ij} and Υ for a given isobaric section. Unfortunately, apart from the region of heavy nuclides there are only a few instances in which two mass differences are known for odd isobars.

In order to make some use of the extensive data corresponding to odd mass isobars for which only one mass difference is known, one may for these cases as a reasonable first approximation let $r^{ij} = 1$ (See GE, Fig. 5) and solve this one equation for Υ .

In Fig. 4 is shown the location of the minimum mass points of odd mass nuclides which have been computed using a recent collection of beta decay energies (circles) and a set of mass values[16] (squares). This true minimum of the valley has been computed by N. J. Marucci.[17] This work is also incorporated in a paper by Nader, Marucci and Green.[18] In these papers the parameter φ_v indicates the true minimum of the valley.

Also shown in Fig. 4 is the difference $\Upsilon = D_m^{ij} - D_m^r(A)$ computed using Eq. (5.8) and Eq. (5.10). It is clear from the plot that in the main the experimental points do fluctuate in accordance with the predictions based upon the reference shell function. The agreement may by improved even further if in the heavy region $D_m(A)$ were taken as the dotted curve indicated in Fig. 4.

7. Shell Correction and the Nuclear Masses.

The constants, k_{ij} , in Eq. (5.3) are still to be determined. Substituting S_{ij} from Eq. (5.3) into Eq. (2.3), then

$$R(N,Z) = -\bar{\alpha}_i (N - \bar{N}_i)^2 - \bar{\alpha}_j (Z - \bar{Z}_j)^2 + k_{ij} + J^0 \Theta^{0^2} + P . \qquad (7.1)$$

For odd mass beta stable nuclides the pairing term and parabolic term will be small so that the constants, k_{ij} , can be evaluated approximately by substituting the data appropriate for these nuclides. Using the

values of $\bar{\alpha}_i$, $\bar{\alpha}_j$, $\bar{N}_i$ and $\bar{Z}_j$, from Table II as well as a table of $R(N,Z)$ values computed from recent mass data the various k_{ij} values have been calculated. In this computation it has been noted that for a particular zone, i.e., a specific i and j, the computed values of k_{ij} varied somewhat. The k_{ij} at shell edges deviated the greatest from the average; accordingly, values of $R(N,Z)$ for either magic N or magic Z or both were not included in the final computation of k_{ij}. The values of k_{ij} so calculated check rather closely with a set obtained by a graphical method. The estimated values of k_{ij} are listed in Table III. To test this set of k_{ij} values and the remainder of the shell correction, the following function is plotted in Fig. 5

$$\Delta^{ij}_m(A) - \Delta_m(A) = -\frac{1}{N_u - N_l}\left[N_m(A) - \frac{N_u + N_l}{2}\right]^2 - \frac{1}{Z_u - Z_l}\left[Z_m(A) - \frac{Z_u + Z_l}{2}\right]^2$$

$$+ k_{ij} - \frac{1}{4J^{ij}(A)}\left\{\frac{1}{N_u - N_l}\left[N_m(A) - \frac{N_u + N_l}{2}\right] - \frac{1}{Z_u - Z_l}\left[Z_m(A) - \frac{Z_u + Z_l}{2}\right]\right\}^2 . \quad (7.2)$$

The function represented by Eq. (7.2) is discontinuous at the magic numbers. These discontinuities are probably not entirely significant, since the shell term is expected to be inaccurate at these shell edges. If in following the atomic model, one had joined a nuclide corresponding to a closed shell with a straight line segment to the nuclide with a closed shell plus one neutron or proton in the curves for $-\partial S_{ij}/\partial N$ and $-\frac{\partial S_{ij}}{\partial Z}$, one would have avoided these discontinuities.[19] The residual masses of beta-stable odd-mass nuclides should fall fairly close to this curve except at shell edges. On the other hand, the beta-stable even-mass nuclides, which is included because there are not enough odd-mass nuclides to test the curve, should fall somewhat below (~ 1 mMU.)

the curve representing Eq. (7.2). An examination of Fig. 5 shows that on the whole these features are borne out by the evidence. The magnitude of the scattering of the points is probably greater than can be attributed to experimental error, to the pairing effect or to the parabolic effect. Thus unquestionably there is room for improvement in the shell stabilizing.

8. The Shell Correction and Q-Values.

Accepting Eq. (5.3) as the shell correction, it will be of interest to investigate reactions with the target and product nuclides in the same zone. The Q-value for the shell correction, Q_s , is defined as

$$Q_s = S_{ij}(N,Z) - S_{ij}(N+\Delta N, Z+\Delta Z) \quad , \qquad (8.1)$$

from Eq. (2.5). $\Delta N = n - n'$, $\Delta Z = z - z'$ where n , n' , z , z' are the neutron and proton numbers of the incident and ejected particles, respectively. Substituting the expression for S_{ij} , Eq. (8.1) becomes

$$Q_s = 2\alpha_i (n-n')(N-\tilde{N}_i) + \alpha_i (n-n')^2 + 2\alpha_j (z-z')(Z-\tilde{Z}_j) + \alpha_j (z-z')^2 \quad . \qquad (8.2)$$

Using the simplified set of constants [Eq. (5.10)], this becomes

$$Q_s = 2(n-n')(N-\bar{N}_i)/(N_u-N_l) + 2(n-n')^2/(N_u-N_l) + 2(z-z')(Z-\bar{Z}_j)/(Z_u-Z_l) + 2(z-z')^2/(Z_u-Z_l) \quad , \qquad (8.3)$$

an equation which is quite simple to handle. To test the accuracy of the complete reference surface, Q-values of numerous (γ,n) and alpha decay reactions have been computed. Upon comparing these predicted

values with the (γ,n) threshold values given by Sher,[20] and the α -decay energies given by Perlman and Seaborg,[21] one finds that 67% of the predictions are within 1 mMU of the experimental value. This represents a substantial improvement in accuracy with respect to predictions based upon the smooth reference function alone, or the semi-empirical mass functions.

Conclusions

The study of the discontinuities of the experimental mass surface led to certain conclusions regarding pairing discontinuities and shell discontinuities.

The frequently accepted assumption that pairing effects may be represented by $+H(A)$, $-H(A)$, and zero for OO, EE, and OE-EO nuclides, respectively, where H(A) is $36/A^{3/4}$ or $140/A$ has been examined. This assumption is found to be untenable for the following reasons: (1) These functions exaggerate the average magnitude of the pairing effect for light nuclides. The function $12/A^{1/2}$ probably furnishes a closer representation of the average magnitude of the pairing effect. (2) The additional energy of unpaired neutrons or unpaired protons with respect to even N even Z nuclides differs in many regions, i.e. frequently $\pi \neq p$. (3) In some regions the energies associated with unpaired particles are non-additive. This suggests that an appreciable pairing interaction is present in OO type nuclides.[22] (4) The expressions for the pairing effect involving shell quantum numbers which were derived by Mayer using the shell model are not inconsistent with the available evidence. In view of the many successes of the shell model, it would seem that the final pairing correction will of necessity embody shell quantum numbers and hence will not be representable as a simple function of A, N, or Z.

In the study of the shell discontinuities evidence is found that the shell effect upon neutron and proton binding energies may be approximately represented by a series of straight line segments between major magic numbers. This representation is also suggested by the general nature

of the discontinuities in atomic ionization energies. Because the available data and the method of analysis did not permit a precise assignment of the parameters which characterize these straight line segments, the consequences of a uniquely defined set of straight line segments was studied. These segments were found to be a reasonable representation of the available evidence. Pursuing this representation, a shell stabilizing correction to nuclear energies was deduced which gives a rather good account of the departures from the general trends of beta stability, nuclear masses, and nuclear Q-values.

Perhaps the most startling conclusion to which one is led from this approximate representation is the large variation of masses which may be identified with a shell stabilizing term. The fact, that in most regions where accurate mass values are available, the line of beta stability cuts the corners of shell zones, has tended to obscure this feature of the experimental mass surface. Only in the heavy region does one meet a situation where the true range of the shell correction can be gauged from the doubly magic corner of the zone to the peak. How the reference line of beta stability (which is a fairly good one) crosses with respect to zones defined by magic N and magic Z numbers is indicated in Fig. 6. It may be concluded, therefore, that shell effects do greatly distort the masses of beta stable nuclides from what they would be in the absence of shell effects. Accordingly, theoretical expressions based upon the statistical theories of the nucleus must be adjusted to mass values which are substantially different from the actual masses of nuclides.

Unquestionably a better representation can be found for the shell

stabilizing term than our present one. The local adjustment of the parameters incorporated in Eq. (5.3) probably would lead to a substantial improvement. It is also probable that the true shell correction may embody semi-magic numbers and curved segments. At this time, the experimental data is too sparse and too inaccurate in many regions of the mass surface to offer great encouragement to an effort to refine the shell correction on the basis of purely empirical considerations. Of necessity, such a study will be a tedious one since it will have to be made in conjunction with a more precise representation of the smooth trends of the nuclear mass surface and a more precise representation of the pairing effect than the simple expressions which have been used here thus far. It appears, therefore, that a point has been reached at which one might best look to current nuclear theories to find a better representation of the shell stabilizing term.

9. First Atomic Ionization Potentials.

The first ionization potentials in the atomic case[23] are analogous to the binding energies of the last nucleon for the nuclear case.[23] There are definite similiarities in the diagrams of the atomic ionization potentials[15] and the neutron and proton binding energies, Figs. 1 and 2, respectively. Electron, neutron or proton binding energies can be represented approximately by straight line segments rising from a minimum at the opening to a maximum at the close of the particular shell. In the remainder of this paper an investigation of the saw-toothed ionization potential curve is made. It is advantageous to study the atomic case for several reasons: (1) The electron-nucleus interaction is known to be chiefly coulombic; (2) There are available several statistical models which describe the atom fairly well. In addition, this is an important study since no quantum mechanical analysis exists for these energy values, at least none has been published. This is concluded from a search of the literature. A successful description of the ionization potentials of the atom might serve as a guide in the study of nuclear shell structure.

F. Rasetti[24] has used the Fermi statistical gas model of the electrons to successfully predict the M_3 x-ray levels for the atom. Fermi[25] has followed his origional paper on the statistical electron gas by using this model to calculate the Rydberg correction to the s term. In a more recent paper, Gáspár[26] has used the Fermi-Thomas potential to express the effective nuclear charge of the atom. This he approximates by a universal function. The universal function he then approximates

by a simple analytical expression that can be used to solve the one-electron Schrödinger equation. This he solves for the eigenfunctions and energies of electrons in the deepest s, p, d, and f energy states. The x-ray energies found in this way are in good agreement with the experimental values.

Each of these writers has assumed the electrical potential in the interior of the atom to be described by the Fermi-Thomas potential, function $\varphi(x)$, which is a solution of the equation

$$\varphi''(x) = \varphi^{3/2}(x)\, x^{-\frac{1}{2}} \quad .$$

In this equation x is a dimensionless parameter defined by $x = \frac{r}{\mu}$, with $\mu = 0.8853 a_0 Z^{-\frac{1}{3}}$ taken as the unit of length. $\varphi(x)$ is the ratio of effective nuclear charge to the charge on the nucleus. The potential energy, $V(r)$, is then given by the function

$$V(r) = -\frac{Ze^2}{r}\varphi\left(\frac{r}{\mu}\right) \quad .$$

In principle, it is then possible to evaluate the energy of the quantum states of electrons in any atom.

The Fermi-Thomas equation, however, has not been solved in analytical form. It has been solved by Bush and Caldwell[27] by means of a differential analyser. The function $\varphi(x)$ is given in tabular form and hence the potential, $V(r)$, as given is of little value. A means to bypass this difficulty is to express the $\varphi(x)$ approximately by a simple analytical function $\varphi_0(x)$. The form of this approximate function $\varphi_0(x)$ must be such that the Schrödinger equation with $V(r) = -\frac{Ze^2}{r}\varphi_0\left(\frac{r}{\mu}\right)$ can be solved. Gáspár expresses the approximate solution of the Fermi-Thomas equation by the universal function[28]

$$\varphi_0(x) = \frac{e^{-\lambda_0 x}}{1 + A_0 x} \quad , \text{ where } \quad \lambda_0 = 0.1837 \quad \text{and} \quad A_0 = 1.05 \quad .$$

Since this does not give a potential that leads to closed solutions of

the Schrodinger equation, it must also be approximated. Both Rasetti and Gaspar in their solutions of the one-electron Schrodinger equation express the approximate potential energy in the form

$$U = -\frac{Z^* e^2}{r} - \frac{1}{2}\frac{\lambda e^2 a_0}{r^2} - K_0 \quad . \tag{9.1}$$

a_0 is the Bohr radius and Z^*, λ, K_0 are arbitrary constants. These constants are evaluated in such a way that at the point r_m, where $r^2|\psi(r)|^2$ has a maximum, the true[29] and the approximate potential, Eq. (9.1), and their first and second derivatives agree. Rasetti used a graphical method to determine the distance r_m. To determine the value of r_m by the method of Gáspár, one must solve extremely complicated transcendental equations. Without the aid of some sort of automatic computing device, this would be an arduous task. Once the values of r_m are found, however, the eigenfunction and eigenvalues follow easily. For larger radial quantum numbers the task becomes more difficult and somewhat arbitrary. The function $r^2|\psi(r)|^2$ no longer will have a single peak but will have several depending on this radial quantum number. An ambiguity or arbitrariness arises as to which r_m to use.

For the solution of the Schrodinger wave equation, Rasetti and Gaspar accept the angular dependence of the one-electron ψ, to be just the usual spherical harmonics, $Y_l^{|m|} = P_l^{|m|}(\cos\theta)\, e^{im\varphi}$. The radial equation is then of the form

$$\frac{1}{r^2}\frac{d}{dr}\left(r^2\frac{dR(r)}{dr}\right) + \left[\frac{2\mu}{\hbar^2}(W-U) - \frac{l(l+1)}{r^2}\right]R(r) = 0 \quad . \tag{9.2}$$

The solution to Eq. (9.2) as given by these two, using the approximate potential Eq. (9.1), is of the hydrogenic form, $R(r) = A r^{n^*-1} e^{-\beta r}$,

where $n^* = \frac{1}{2}\left\{\left[1 - 4\lambda + 4l(l+1)\right]^{1/2} + 1\right\}$ and $\gamma = \frac{Z^*}{n^* a_0}$. The energy eigenvalues are

$$W = -\tfrac{1}{2}\gamma^2 e^2 a_0 - \chi_0 \quad . \tag{9.3}$$

The potential Eq. (9.1) represents a combination of an inverse-cube and an inverse-square central force. The case of the inverse-square force (i.e., $\lambda = 0$) is just the familiar hydrogen-like atom problem with well behaved solutions in terms of the associated Laguerre polynomials. The case of the inverse-cube force alone ($Z^* = 0$) has been fully treated by Shortley.[30] Shortley concludes that for the inverse-cube force, although solutions for negative energy exists that satisfy the usual boundary conditions, they cannot be admitted because the Hamiltonian is not Hermitian in these solutions. The solutions to this equation are in the form of Bessel functions. The energy occurs in the argument and hence there is no quantization. The equation solved by Rasetti and Gáspár, Eq. (9.2), is a combination of these two forces. The general case where neither of the central forces can be neglected is considered in chapter 10. The Schrodinger equation is solved with the potential Eq. (9.1) and the conditions on the central force parameters examined.

10. Solution of the Radial Wave Equation.

Solutions of the one-electron Schrödinger equation

$$\frac{1}{r^2}\frac{d}{dr}\left(r^2\frac{dR(r)}{dr}\right) + \left\{\frac{2\mu}{\hbar^2}(W - U) - \frac{\lambda(l+1)}{r^2}\right\} R(r) = 0 \tag{10.1}$$

with

$$U = -\frac{Z^* e^2}{r} - \frac{1}{2}\frac{\lambda e^2 a_0}{r^2} - \chi_0 \tag{10.2}$$

are sought. Putting $\bar{U}(r)$ into Eq. (10.1) and collecting terms, we find

$$\frac{1}{r^2}\frac{d}{dr}\left(r^2\frac{dR(r)}{dr}\right)+\left\{\frac{2\mu}{\hbar^2}(W+\chi_0)+\frac{2Z^*}{a_0}\frac{1}{r}+\left(\lambda-l(l+1)\right)\frac{1}{r^2}\right\}R(r)=0, \quad (10.3)$$

where $\frac{\hbar^2}{\mu e^2}=a_0=$ Bohr radius. Here the interest is only for $W<0$. Let

$$\alpha^2=-\frac{2\mu(W+\chi_0)}{\hbar^2} \quad (10.4)$$

and

$$\beta=\frac{Z^*}{a_0\alpha} \quad (10.5)$$

Replacing $R(r)=S(\rho)$, where $\rho=2\alpha r$, then Eq. (10.3) becomes

$$\frac{1}{\rho^2}\frac{d}{d\rho}\left(\rho^2\frac{dS(\rho)}{d\rho}\right)+\left[-\frac{1}{4}+\frac{\beta}{\rho}+\frac{\lambda-l(l+1)}{\rho^2}\right]S(\rho)=0, \quad (10.6)$$

$$0\le\rho\le\infty .$$

This equation can be reduced to the hypergeometric form, i.e. to a form that involves only a two term recurrence relation for a power series type solution, by the substitution $S(\rho)=e^{\pm\rho/2}F(\rho)$. By the condition that the solutions be quadratically integrable, the only acceptable substitution is $S(\rho)=e^{-\frac{\rho}{2}}F(\rho)$. Putting this into Eq. (10.6), the equation takes the hypergeometric form

$$\frac{d^2F(\rho)}{d\rho^2}+\left(\frac{2}{\rho}-1\right)\frac{dF(\rho)}{d\rho}+\left\{\frac{\beta-1}{\rho}+\frac{\lambda-l(l+1)}{\rho^2}\right\}F(\rho)=0 . \quad (10.7)$$

The solution to this equation is assumed to have the form of the power series $F(\rho)=\rho^s\sum_{\nu=0}^{\infty}a_\nu\rho^\nu$, $a_0\neq 0$. The recurrence relation becomes then

$$\{(s+\nu+1)(s+\nu+2)+\lambda-l(l+1)\}a_{\nu+1}=\{s+\nu+1-\beta\}a_\nu \qquad (10.8)$$

and

$$s(s+1)+\lambda-l(l+1)=0 \qquad (10.9)$$

is the indicial equation. An investigation of the power series for large ν shows that the expansion behaves as

$$\frac{a_{\nu+1}\rho^{\nu+1}}{a_\nu\rho^\nu}=\frac{(s+\nu+1-\beta)\rho}{(s+\nu+1)(s+\nu+2)+\lambda-l(l+1)}\longrightarrow\frac{\rho}{\nu}$$

This is the same as the ratio of the $(\nu+1)^{th}$ to ν^{th} term of e^ρ and hence the series does not converge for large values of ρ. This requires that the series terminates after some ν, say $\nu=n'$, i.e. $a_{n'}\neq 0$ but $a_{n'+1}=0$. All other terms for $\nu>n'$ will vanish because of the relation Eq. (10.8). Then $s+n'+1-\beta=0$ or $\beta=n^*$, where $n^*=s+1+n'$.

The roots of the indicial equation, Eq. (10.9), are

$$s=-\tfrac{1}{2}\pm\left[(l+\tfrac{1}{2})^2-\lambda\right]^{1/2}, \text{ then}$$

$$n^*=n'+\tfrac{1}{2}\pm\left[(l+\tfrac{1}{2})^2-\lambda\right]^{1/2}. \qquad (10.10)$$

n' is called the Radial Quantum Number just as in the hydrogen atom problem and n^* the Reduced Total Quantum Number.

The magnitude of the constant λ determines the effect of the inverse-cube central force. It is assumed that it can have any value from + to - infinity. As an example, for a large positive value of λ, $\lambda>>z^*$, the force of interaction would be predominately an attractive inverse-cube force. As the valence electron comes closer to the nucleus,

The shielding due to the electron cloud about the nucleus has less effect. It is therefore necessary to expect a small attractive inverse-cube force in addition to the inverse-square force. This requires that λ be positive. The fact that the potential, $U(r)$, goes to infinity at the origin is no serious objection because of the finite size of the nucleus. For $Z \gtrsim 10$ only those electrons that are closest to the nuclear surface will experience the effects of the inverse-cube force.

Eq. (10.10) reduces to the special cases of Gáspár, $n'=0$, and Rasetti, $n'=0$, $l=2$, provided $(l+\frac{1}{2})^2 > \lambda$ and the upper sign (+) is taken. Also for these conditions the energy has the form Eq. (9.3).

For the case that $\lambda > (l+\frac{1}{2})^2$, then Eq. (10.10) can be written as

$$n^* = n' + \tfrac{1}{2} \pm i\left[\lambda - (l+\tfrac{1}{2})^2\right]^{1/2}$$

so that

$$n^* - n' + \tfrac{1}{2} \pm i\left[\lambda - (l+\tfrac{1}{2})^2\right]^{1/2} = 0 . \qquad (10.11)$$

This requires that the real and imaginary parts of Eq. (10.11) vanish identically. That means that $\lambda = (l+\frac{1}{2})^2$; but, it was assumed that $\lambda > (l+\frac{1}{2})^2$. Since it is not possible for a number, λ, to be equal to and simultaneously greater than the same number, $(l+\frac{1}{2})^2$, there is a contradiction. It is concluded then that in order to have bound states that give quantized energy values for a potential of the form, Eq. (9.1), it must be true that $\lambda < (l+\frac{1}{2})^2$.

The only restriction on the constant χ_0 is that it be small since a boundary condition on the potential is that $U(\infty)$ vanish. For the low lying states this small χ_0 can be tolerated.

11. Fermi-Thomas Model to Predict Ionization Potentials.

The successes of the Fermi-Thomas gas model to predict the x-ray energy levels[23,25] and Rydberg correction[24] suggest that this model might also be used to calculate the ionization potentials of the valence electrons.

For these calculations a universal function for the reduced effective nuclear charge Z_p/Z is assumed. This is taken to be of the form of a polynomial for which the interaction will involve an inverse-quadratic force in addition to the inverse-square and cube forces,

$$Z_p/Z = \varphi_1(x) = c_1 x + c_0 + c_{-1}\frac{1}{x} + c_{-2}\frac{1}{x^2} \quad , \qquad (11.1)$$

where the distance from the nucleus is measured in the unit of length $\mu = 0.8853\, a_0 Z^{-\frac{1}{3}}$ and the c_i are empirical constants. This form has the advantage that the difficulties involved in finding by the methods of Rasetti and especially of Gáspár are avoided. The arbitrariness arising for states with intermediate radial nodes, i.e. $n' > 0$ will also be missing.

The electrical potential for the valence electrons is taken as

$$V = -\frac{e^2}{r}\left[1 + (Z-1)\,\varphi_1\left(\frac{r}{\mu}\right)\right] \quad . \qquad (11.2)$$

This is the form of the potential that was used by Rasetti. The valence electron is assumed to be in the field of a singly ionized atom. The ion of nuclear charge Z is considered as a neutral atom of charge $Z-1$ plus an extra proton in the nucleus, thus μ is evaluated for $Z-1$. This leads then to the form Eq. (11.2).

The Schrödinger equation with the potential given by Eq. (11.2) and Eq. (11.1) cannot be solved directly and hence an approximation to this

potential is made. In order to take full advantage of previous work, the potential energy in the zero order approximation is taken as the coulomb-type potential

$$V_0 = -\frac{Z^* e^2}{r} \quad . \tag{11.3}$$

Z^* will be referred to as the effective nuclear charge and is taken as a function of the atomic number. The solutions of the Schrödinger equation are just the familiar hydrogenic functions with Z replaced by Z^*.[31] Since this method has been designed to give only the gross affect of the energy levels, it will be assumed that the wave functions, ψ_m and energy values W_n correspond to non-degenerate solutions of the hydrogenic wave equation. The energy values are given by

$$W_n = -\frac{\mu e^4 Z^{*2}}{2\hbar^2 n^2} = -\frac{e^2}{2a_0}\frac{Z^{*2}}{n^2}$$

$$= -13.6\,\frac{Z^{*2}}{n^2} \quad \text{(e.v.)} \quad . \tag{11.4}$$

In general, the approximation Eq. (11.3) can be improved upon by treating the difference, $U = V - V_0$, as given by Eqs. (11.1), (11.2) and (11.3), as a perturbation term added to the Hamiltonian. This perturbation will be of the form

$$U = V - V_0 = -\frac{e^2}{r}\left[1 + (Z-1)\,\varphi_{Z-1}\left(\frac{r}{\mu}\right)\right] + \frac{Z^* e^2}{r}$$

$$= \frac{e^2}{r}\left[(Z^*-1) - (Z-1)\,\varphi_{Z-1}\left(\frac{r}{\mu}\right)\right] \quad . \tag{11.5}$$

In terms of the universal function, Eq. (11.1), with $r = \mu x$, this becomes

$$U = -\frac{c_1 e^2 (Z-1)^{4/3}}{.8853\, a_0} + \left[(Z^*-1) - c_0(Z-1)\right]\frac{e^2}{r} - c_{-1}.8853\, a_0 (Z-1)^{2/3} e^2 \frac{1}{r^2}$$

$$- c_{-2}(.8853\, a_0)^2 (Z-1)^{1/3} e^2 \frac{1}{r^3} \quad . \qquad (11.6)$$

The perturbation U will cause a change in the energy value Eq. (11.4) by an amount w .[32] The energy values to the first order approximation are just

$$W = W_n + w \quad , \qquad (11.7)$$

where $w = (\psi_m, U\psi_m)$.

With U in the form Eq. (11.6), the integrals, $w = (\psi_m, U\psi_m)$, can be easily calculated. They involve just expectation values of r^{-s} $(s = 1,2,3)$. These averages have been computed by Van Vleck[33] for the case of an inverse-square central field for s from 1 to 6. Those that are used in this thesis are tabulated below.

$$\langle r^{-1}\rangle = \frac{Z^*}{a_0 n^2} \quad , \quad \langle r^{-2}\rangle = \frac{Z^{*2}}{a_0^2 n^3 (l+\tfrac{1}{2})} \quad , \quad \langle r^{-3}\rangle = \frac{Z^{*3}}{a_0^3 n^3 l(l+\tfrac{1}{2})(l+1)} \quad . \qquad (11.8)$$

The average value of r^{-3} for s - waves is infinite and for that reason only states for $l > 0$ are considered here.

The final form of the universal energy formula is:

$$W = W_n + w_n$$

$$= -13.6\frac{Z^{*2}}{n^2} - \frac{c_1 e^2 (Z-1)^{4/3}}{.8853\, a_0} + \left[(Z^*-1) - c_0(Z-1)\right]\frac{e^2}{a_0}\frac{Z^*}{n^2}$$

$$- c_{-1}.8853\,(Z-1)^{2/3}\frac{e^2 Z^{*2}}{a_0 n^3 (l+\tfrac{1}{2})} - c_{-2}(.8853)^2\frac{(Z-1)^{1/3} e^2 Z^{*3}}{a_0 n^3 l(l+\tfrac{1}{2})(l+1)} \quad . \qquad (11.9)$$

The effective nuclear charge function, $Z^*(Z)$, must be of such a form that Z^* reduces to unity for the case of the hydrogen atom. It is convenient to take $Z^*(Z)$ to be of the form $Z^* = 1 + \alpha(Z-1)$. This form is also suggested by equating the potentials Eq. (9.1) and Eq. (11.2), their first and second derivatives at some value of $r = \bar{r}$. This reduces to the necessary form for the case of the hydrogen atom, i.e. $Z^* = 1$ for $Z = 1$. The constant α has been chosen from a consideration of the energy level diagram of the Boron group, see for example Fig. 8.1, White, Introduction to Atomic Spectra, Mc Graw-Hill (1934). In this way α was found to be approximately .050. Hence, the effective nuclear charge for all the atoms in the periodic system is assumed in the zeroth approximation to be given by

$$Z^* = 1 + .050(Z-1) \quad . \qquad (11.10)$$

The constants c_i can also be chosen in a systematic way. The average values of r^{-s}, Eq. (11.8), do not have the same relative weights for the various l-waves. In Table IV values of functions proportional to those of Eq. (11.8) for various Z are listed. From the values for $\langle r^{-1} \rangle$, one sees the waves for larger l (f especially) have the greater relative weights. The relative weights of the $\langle r^{-2} \rangle$ terms are roughly the same for all the l - waves while those for $\langle r^{-3} \rangle$ are greater for the p -waves. Using these characteristics, the constants c_i were chosen such that the corresponding W gave the optimum fit of the experimental data. The so obtained are

$$c_1 = -.00036 \ , \ c_0 = .035 \ , \ c_{-1} = .074 \ , \ c_{-2} = 0.40 \quad . \qquad (11.11)$$

Using these values of c_i , the resulting ionization energies have been computed. It is necessary to compute only the ionization potentials of the first and last element in any particular shell and join these by a straight line. This is approximately so since within a shell the variation of the energies, W_n and ω , is very nearly linear with the atomic number. A good example of this variation is the 4 shell in Fig. 7. The ionization energies are compared to the experimental values in Fig. 7. The ionization potentials for $A<10$ have not been computed because of the statistical nature of the atomic core considered.

From a consideration of the simple form of the parameters involved (eg. Eq. (11.10)) and the case with which the values can be computed, the agreement in Fig. 7 is rather good.

There may be some objection to the perturbation method used here in that a first order approximation for some waves is not sufficient. For the f-waves especially, the perturbation energy, ω , is approximately 50% of W_n . This is also true for the higher d-waves. It must again be emphasized that this theory should not be taken as complete. It has been designed to give only the gross effects of the energy levels and hence perturbations beyond the first order are not considered.

The advantage of a theory such as this is the simple form of the parameters. Here the experimental data has been described in terms of five empirical constants (α and c_i). The energy values can then be computed easily in a short time for every element in the periodic system.

In Fig. 8 are plotted the solution of the Fermi-Thomas equation as given by Bush and Caldwell as well as the function Eq. (11.1) with the

constants Eq. (11.11). From this it is concluded that experiment requires that the potential function has a singularity at the origin and approaches zero slower than the Fermi-Thomas potential function. The singularity at the origin could have been avoided by assuming a universal function that approaches a finite value at the origin. A Kerner power series type potential[34] or a Morse type potential[35] satisfy this condition and could be used as good approximations to the Fermi-Thomas potential. These are, however, as difficult to use as the universal function of Gáspár and hence, they are of little advantage. This singularity at the origin is not serious because of the finite size of the nucleus as stated before in regards to the approximation Eq. (9.1).

12. Excited States.

A criterion for a successful atomic model might be the ability to predict the first few excited states of the valence electron in addition to the x-ray levels and excitation energies. The statistical model of Fermi-Thomas, however, should not be expected to do this. This model assumed the electrons to be represented by a completely degenerate gas and hence, excited states should not be considered. The atomic model presented in this thesis is a combination of a statistical and an independent particle model. It was thought that an atomic model of this form would predict the low lying excitation energies. The first few excitation energies of the elements listed in Table IV, which do not involve S -waves, have been computed and are listed in Table V. Also in this table are the corresponding experimental values as given by R. F. Bacher and S. Goudsmit, Atomic Energy States, Mc Graw-Hill (1932).

The energy levels for S -waves were left vacant in this table because of the infinity arising in the evaluation of the perturbation energies.

Several interesting results are noted in Table V. The atomic model presented in this thesis predicts for the cases A = 37, 39, 46, 57, 79, that the excited states are more stable than the ground state. The ground state is found to be more stable, as it should be, for all the other elements considered. For those cases which the ground state is more stable, the energy difference between the states of an atom agree roughly with experiment in only a few cases. These are considered fortuitous. It is to be expected that the agreement with experiment will be no better for those elements not lying at the shell edges. Hence, this atomic model, in general, will not predict the excited levels accurately. It can perhaps be concluded that this model has done as well as might be expected with the statistical nature of the potential of the outermost electron. Better agreement with experiment might be made by considering a potential for the valence electron that incorporates in itself irregularities due to shells, such as is found by the Hartree-Fock self-consistent method.

Conclusions.

In the second part of this thesis an attempt to find a quantum mechanical representation of the corresponding electronic shell stabilizing term was made. A theory such as this has enormous possibilities since a successful description of the ionization potentials of the atom might serve as a guide in the study of nuclear shell structure. The study of the atomic ionization potentials has led to certain conclusions regarding the form of the force field of the electron-nucleus interaction.

The atomic model was taken to be a combination of a statistical and an independent particle model, the potential of the valence electron being taken as a smooth function of the atomic number.

The potential energy expressed as a combination of an inverse-square and inverse-cube central force has been examined. It is concluded that in order to have an atomic model that will correspond to bound states and quantized energy levels, certain conditions must be imposed on the central force parameters. The admixture of the inverse-cube force must be such that λ in Eq. (9.1) is positive and is less than $(l + \frac{1}{2})^2$. This insures that the force field is such as to give bound as well as quantized energy states for the electron.

To compute the excitation energies the potential energy was taken in the first approximation to be of coulombic type. The eigenfunctions and eigenvalues are then just the hydrogenic eigen functions and eigenvalues. A better approximation was made using a perturbation method. The agreement with experiment is only fair. The low lying excitation energies were also computed using this model. There was slight agree-

ment with experimental values, and it is concluded that this model will not predict excitation energies.

From this analysis of the atomic ionization energies, the following things might be concluded: (1) On the basis of a smooth function, $V(r)$ for the outermost electron, the results are perhaps as good as might be expected. On the basis of this function, a fair representation is obtained of the ionization energies of the atom. (2) The inaccuracies might be attributed to: (a) the real effective potential function for the outermost electron probably has shell irregularities itself; (b) the perturbation method used can possibly be improved upon; (c) effects due to exchange and spin-orbital coupling have been neglected.

The writer would like to thank Alex E. S. Green for suggesting this thesis and for his guidance towards its completion. The part of this work which concerns the nuclear mass surface was initiated several years ago by Professor Green and contributions to this study were made by many of Professor Green's students and assistants, particularly: R. B. Minogue, N. J. Marucci, R. Oppenheim, J. S. Nader, N. Engler, R. Oswald and Mrs. W. Steiger. The writer, therefore, wishes to acknowledge his indebtedness to the above persons as well.

1. D. R. Hartree, Proc. Camb. Phil. Soc. 24, 89 (1928)

2. C. F. von Weizsäcker, Zeits. f. Physik 96, 431 (1935)

3. Alex E. S. Green, Phys. Rev. 86, 654 (1952)

4. A complete description of this mass surface is given in a manuscript by A. E. S. Green, Nuclear Physics, Mc Graw-Hill (to be published) and Professor Green's Nuclear Physics Class lecture notes.

5. It is conventional to represent the nuclear type by two letters. The first refers to the neutron, the last the proton. Thus, for example, an EO type refers to a nucleus with an odd number of neutrons and an even number of protons.

6. A. E. S. Green and N. A. Engler, Phys. Rev. July 1, 1953, to be published, hereafter referred to as GE.

7. National Bureau of Standards, U. S. Circular 499. Nuclear Data and Supplements appearing in Nuclear Science Abstracts.

8. This can be seen by referring to Eqs. (3.5) and (3.1) for the case of the neutron and the analogous equations for the proton.

9. C. D. Coryell and H. E. Suess, Phys. Rev. 86, 609 (1952)

10. S. Glasstone, Source Book on Atomic Energy, D. Van Nostrand Co. Inc. (1950). The pairing function suggested by J. W. Blatt and V. F. Weisskopf in, Theoretical Nuclear Physics, Wiley (1952) is quite close to this one.

11. E. Fermi, unpublished

12. M. G. Mayer, Phys. Rev. 78, 22 (1950)

13. P. F. A. Klinkenberg, Rev. Mod. Phys. 24, 63 (1952)

14. C. D. Coryell, Manuscript submitted for publication in Vol. II of Annual Reviews of Nuclear Science, Jan. 1953.

15. See Fig. 98, W. Finkelnburg, Atomic Physics, McGraw-Hill (1950).

16. This set of mass values has been compiled from the recent literature by Alex E. S. Green and various students in the Physics Department at the University.

17. N. J. Marucci, Senior reading thesis, The Line of Beta-Stability, University of Cincinnati (1952).

18. J. S. Nader, N. J. Marucci and A. E. S. Green, Phys. Rev. 86, 654 (1952)

19. A. H. Wapstra, Physica 18, 83 (1952) has proposed a shell stabilizing term which is quite different from that proposed here. The shell stabilizing term has the advantage of introducing sharp breaks in the line of beta stability which is considered to be essential by Coryell (Ref. 14).

20. R. Sher, J. Halpern and A. K. Mann, Phys. Rev. 84, 387 (1951)

21. I. Perlman, A. Ghiorso, G. T. Seaborg, Phys. Rev. 77, 26 (1950)

22. K. Way and M. Wood, Phys. Rev. 86, 608 (1952) have noted an n-p interaction above Pb^{208} which is probably related to this.

23. It should be mentioned here that the reference to the "atomic case" means treating the nucleus as a unit while "nuclear case" has reference to the nucleons as made up of individual particles.

24. F. Rasetti, Zeits. f. Physik 49, 546 (1928)

25. E. Fermi, Zeits. f. Physik 49, 550 (1928)

26. R. Gáspár, J. Chem. Phys. 20, 1863 (1952)

27. V. Bush and S. H. Caldwell, Phys. Rev. 38, 1898 (1931)

28. This is a universal function since once Z is given $\varphi_1(x)$ is determined; $x = 0.8853 a_0 Z^{-1/3}$.

29. The potential involving $\varphi(\varkappa)$ for Rasetti and the universal function, $\varphi_0(\varkappa)$, for Gáspár.

30. G. H. Shortley, Phys. Rev. 38, 120 (1930)

31. Solutions to this problem are tabulated many places in the literature, see for example, Pauling and Wilson, Introduction to Quantum Mechanics, McGraw-Hill (1935), Tables 21.1, 2, 3, 4. This approximation and the resulting perturbation method that follows were suggested to the writer by Professor Green.

32. See for example Section 17.1, Mott and Sneldon, Wave Mechanics and its Applications, Oxford (1948).

33. J. H. Van Vleck, Proc. Roy. Soc. A143, 679 (1934)

34. E. H. Kerner, Phys. Rev. 83, 71 (1951)

35. P. M. Morse, Phys. Rev. 34, 57 (1929)

TABLE I The pairing correction to binding energies

	Neutron binding			Proton binding		
N,Z	$\tau \neq \pi+\nu$	$\tau = \pi+\nu$	$\pi=\nu=$ H	$\tau \neq \pi+\nu$	$\tau = \pi+\nu$	$\pi=\nu=$ H
E,E	ν	ν	H	π	π	H
O,O	$-\tau+\pi$	$-\nu$	-H	$-\tau+\nu$	$-\pi$	-H
E,O	$\tau-\pi$	ν	H	$-\pi$	$-\pi$	-H
O,E	$-\nu$	$-\nu$	-H	$\tau-\nu$	π	-H

TABLE II Shell correction parameters

i	N_l	N_u	α_i	$\tilde{N}$	$\bar{\alpha}_i$	$\bar{N}$
1	0	2			0.300	1
2	2	8	0.22	7	0.1667	6
3	8	20	0.18	18	0.0834	14
4	20	28	0.22	25	0.125	24
5	50	50	0.023	33	0.0455	39
6	82	82	0.022	70	0.0312	66
7	126	126	0.023	104	0.02275	104
8		148	0.048	140	0.0455	137

j	Z_l	Z_u	α_j	$\tilde{Z}$	$\bar{\alpha}_j$	$\bar{Z}$
1	0	2			0.500	1
2	2	8			0.1667	6
3	8	20	0.05	19	0.0834	14
4	20	28	0.088	21	0.125	24
5	28	50	0.023	40	0.0455	39
6	50	82	0.030	53	0.0312	66
7	82	100	0.075	88	0.0555	91

TABLE III Estimated k_{ij} values in mMU.

i,j	2,2	3,2	3,3	4,3	4,4	5,4
k_{ij}	-2.5	2.5	3.0	7.0	3.5	2.5

i,j	5,5	6,5	6,6	7,6	8,7	
k_{ij}	5.5	6.5	8.0	3.5	1.5	

TABLE IV Unperturbed and perturbed energies

Z	nl	Z^*	W_u e.v.	$\frac{Z^*(Z-1)}{n^2}$	$\frac{Z^*(Z-1)^{4/3}}{n^3(l+\frac{1}{2})}$	$\frac{Z^{*3}(Z-1)^{1/3}}{n^3 l(l+\frac{1}{2})(l+1)}$	$.011(Z-1)^{4/3}$	W e.v.
11	3s	1.50	- 3.40					
13	3p	1.60	- 3.87	2.135	.331	.1155	.35	- 4.35
18	3p	1.85	- 5.18	3.50	.559	.2010	.55	- 5.85
19	4s	1.90	- 3.07					
21	3d	2.00	- 6.05	4.45	.436	.0535	.60	- 4.80
29	3d	2.40	- 8.71	7.46	.758	.1035	.95	- 6.82
30	4s	2.45	- 5.10					
31	4p	2.50	- 5.31	4.69	.628	.253	1.02	- 5.65
36	4p	2.75	- 6.44	6.02	.843	.354	1.28	- 7.12
37	5s	2.80	- 4.26					
39	4d	2.90	- 7.15	6.90	.594	.0854	1.40	- 4.62
46	4d	3.25	- 8.99	9.15	.833	.127	1.76	- 5.95
47	5s	3.30	- 5.92					
49	5p	3.40	- 6.30	6.54	.814	.381	1.90	- 6.35
54	5p	3.65	- 7.25	7.75	.995	.487	2.20	- 7.80
55	6s	3.70	- 5.18					
57	5d	3.80	- 7.86	8.52	.675	.1118	2.35	- 4.10
58	4f	3.85	-12.60	13.7	.980	.0815	2.40	- 6.80
63	4f	4.10	-14.30	15.9	1.170	.1011	2.70	- 7.80
64	5d	4.15	- 9.37	10.45	.873	.1515	2.74	- 5.05
65	4f	4.20	-15.00	16.80	1.260	.110	2.80	- 8.30
70	4f	4.45	-16.82	19.2	1.489	.1345	3.10	- 9.40
71	5d	4.50	-11.02	12.6	1.10	.200	3.18	- 6.25
79	5d	4.90	-13.05	15.25	1.40	.2675	3.68	- 7.70
80	6s	4.95	- 9.25					
81	6p	5.00	- 9.45	11.10	1.430	.831	3.80	-10.70
86	6p	5.25	-10.40	12.40	1.644	.980	4.12	-12.35
87	7s	5.30	- 7.80					
89	6d	5.40	-11.00	13.20	1.068	.2160	4.32	- 4.90
91	5f	5.50	-16.45	19.80	1.390	.1418	4.45	- 7.40
95	5f	5.70	-17.68	21.40	1.530	.1600	4.72	- 8.00
96	6d	5.75	-12.45	15.15	1.270	.2678	4.80	- 5.95

TABLE V Excitation energy values (e.v.)

Z	W_0 calc.	W_1 calc.	W_2 calc.	E_0 exper.	E_1 exper.	E_2 exper.
13	- 4.35 (3p)	(4s)	- 3.79 (3d)	- 5.972 (3p)	(4s)	-1.96 (3d)
21	-4.80 (3d)	-3.40 (4p)		- 6.70 (3d)	-4.76 (4p)	
31	-5.65 (4p)	(5s)	-4.50 (4d)	- 5.988 (4p)	(5s)	-1.697 (4d)
36	- 7.12 (4p)	(5s)	- 4.86 (5p)	-13.976 (4p)	(5s)	-2.692 (5p)
37	(5s)	- 5.07 (5p)	- 5.68 (4d)	(5s)	- 2.60 (5p)	-1.77 (4d)
39	- 4.62 (4d)	- 5.54 (5p)		- 6.60 (4d)	-5.25 (5p)	
46	- 5.95 (4d)	(5s)	- 7.42 (5p)	- 8.3 (4d)	(5s)	-4.10 (5p)
49	-6.35 (5p)	(6s)	-5.15 (5d)	- 5.776 (5p)	(6s)	-1.745 (5d)
54	- 7.80 (5p)	(6s)	- 6.28 (6p)	-12.110 (5p)	(6s)	-2.546 (6p)
55	(6s)	- 6.50 (6p)	- 6.17 (5d)	(6s)	-2.469 (6p)	-2.086 (5d)
57	- 4.10 (5d)	- 6.95 (6p)		- 5.72 (5d)	-3.87 (6p)	
79	- 7.70 (5d)	(6s)	-13.75 (6p)	- 9.22 (5d)	(6s)	-8.90 (6p)
81	-10.70 (6p)	(7s)	- 9.68 (7p)	- 6.098 (6p)	(7s)	-3.44 (6p)
86	-12.35 (6p)	(7s)	-11.04 (7p)	-10.730 (6p)	(7s)	-2.531 (7p)

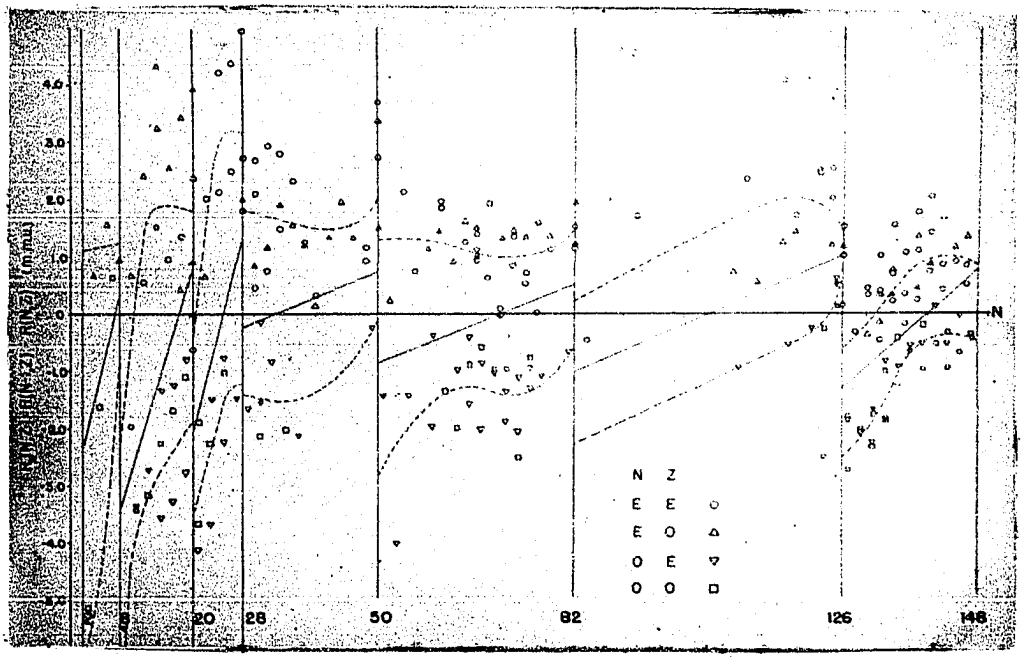

Fig. 1. The residual neutron binding energy vs neutron number. The points are designated as to the type, i.e., the evenness or oddness of the number of neutrons or protons. The grouping of the EE and EO types and the grouping of the OO and OE types can be seen. The dashed curves indicate the average distributions of these groups. The solid line represents our visual estimate of the best straight line representation of $-(\partial S_{ij}/\partial N)$. The $-(\partial S_{ij}/\partial N)$ which we use in Ch. 4 consists of a series of straight line segments running from -1 at the lower magic number to 1 at the upper magic number.

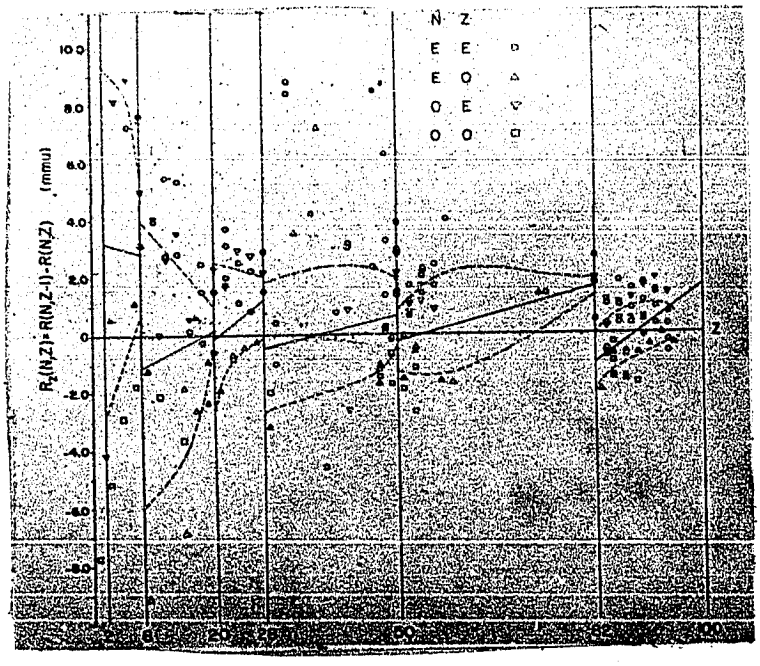

Fig. 2. The residual proton binding energy vs proton number. The points are designated as to the type, i.e., the evenness or oddness of the number of neutron and protons. The grouping of the EE and OE types and the grouping of the OO and EO types can be seen. The dashed curves indicate the average distributions of these groups. The solid line represents our visual estimate of the best straight line representation of $-\left(\partial S_{ij}/\partial Z\right)$. The $-\left(\partial S_{ij}/\partial Z\right)$ which we use in Ch. 4 consists of a series of straight line segments running from -1 at the lower magic number to 1 at the upper magic number.

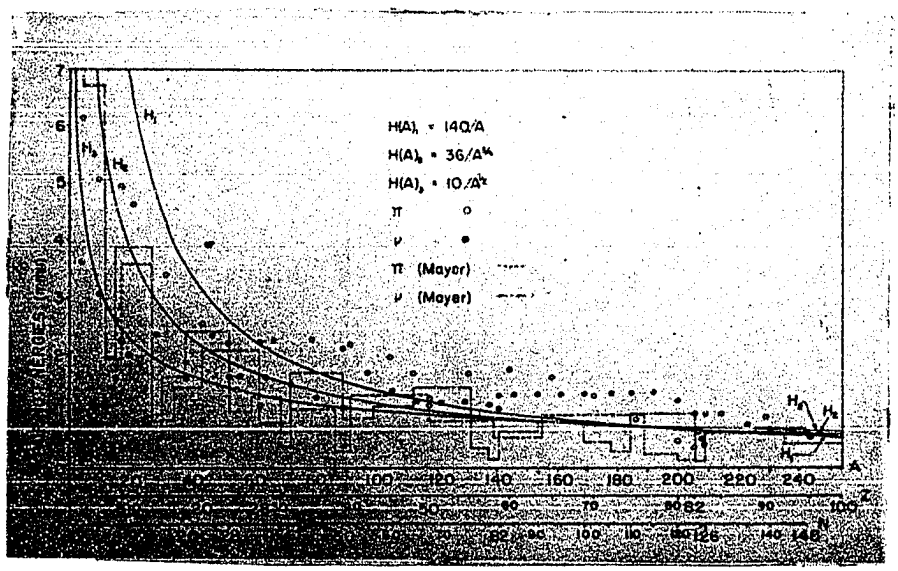

Fig. 3. The pairing energies of the last nucleon are plotted as a function of the mass number. The N and Z scales correspond to values which lie along our reference line of beta stability. The experimental pairing energies (ν and π) as estimated from Figs. 1 and 2 are indicated by the solid circle and square, respectively. The pairing functions of mass number given by Glasstone, Fermi, and Green are represented by the solid curves.

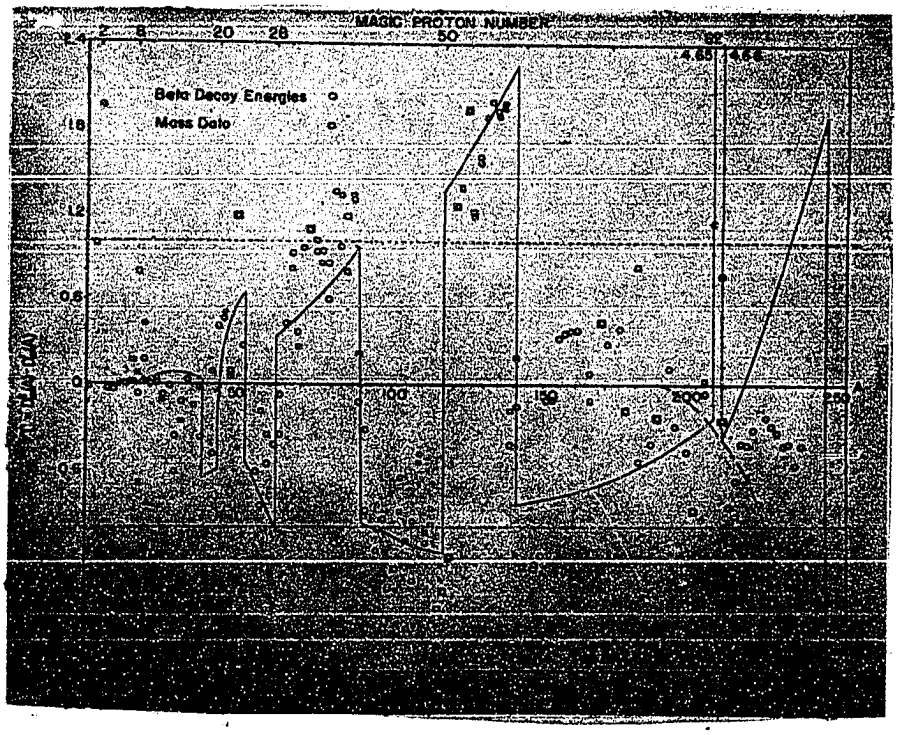

Fig. 4. Location of beta stability point vs mass numbers. The circles and squares indicate the points computed on the basis of experimental data. The solid line represents the line of stability computed on the basis of our reference shell correction and our smooth reference line of beta stability. The dashed line indicates the change in the smooth baseline apparently needed in the very heavy region.

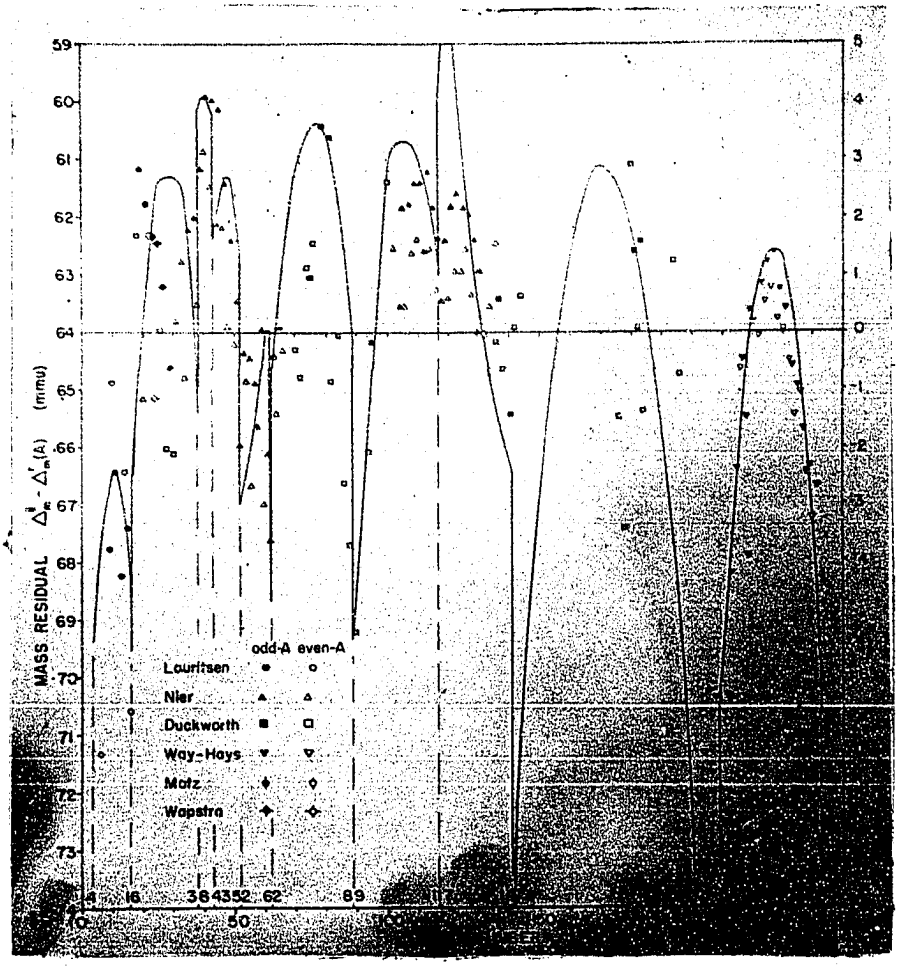

Fig. 5. The mass residuals for beta stable nuclides vs mass number. The solid symbols represent odd-A nuclides and open symbols the even-A nuclides. The symbols used designated the source of experimental data (see references 6-12 in GE). The discontinuous curve represents the mass residuals for the beta stable points of a surface which incorporates our smooth reference functions and our reference shell stabilizing term. The left vertical scale denotes residuals computed with respect to $\Delta^r_m(A) = (A - 100)^2/100$, whereas the right vertical scale denotes residuals computed with respect to $\Delta^r_m(A) = (A - 100)^2/100 - 64$.

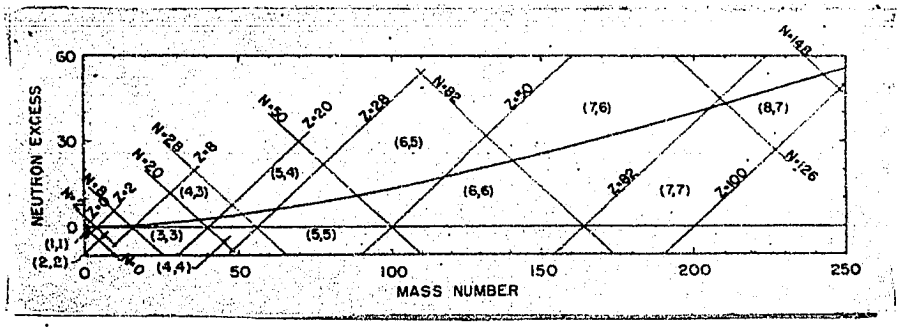

Fig. 6. The line of beta stability in relationship to zones defined by magic numbers. The numbers in parentheses are the indices of the zone (i,j).

Fig. 7. The ionization potentials vs atomic number. The solid circles connected by straight lines represent the experimental values of the first ionization potentials as given by Finklenburg. The open circles connected by the dashed lines represent the ionization potentials computed from Eq. (11.9). The computed points are for the first and last atoms in a particular shell. The crosses represent the first order approximations as computed by Eq. (11.4).

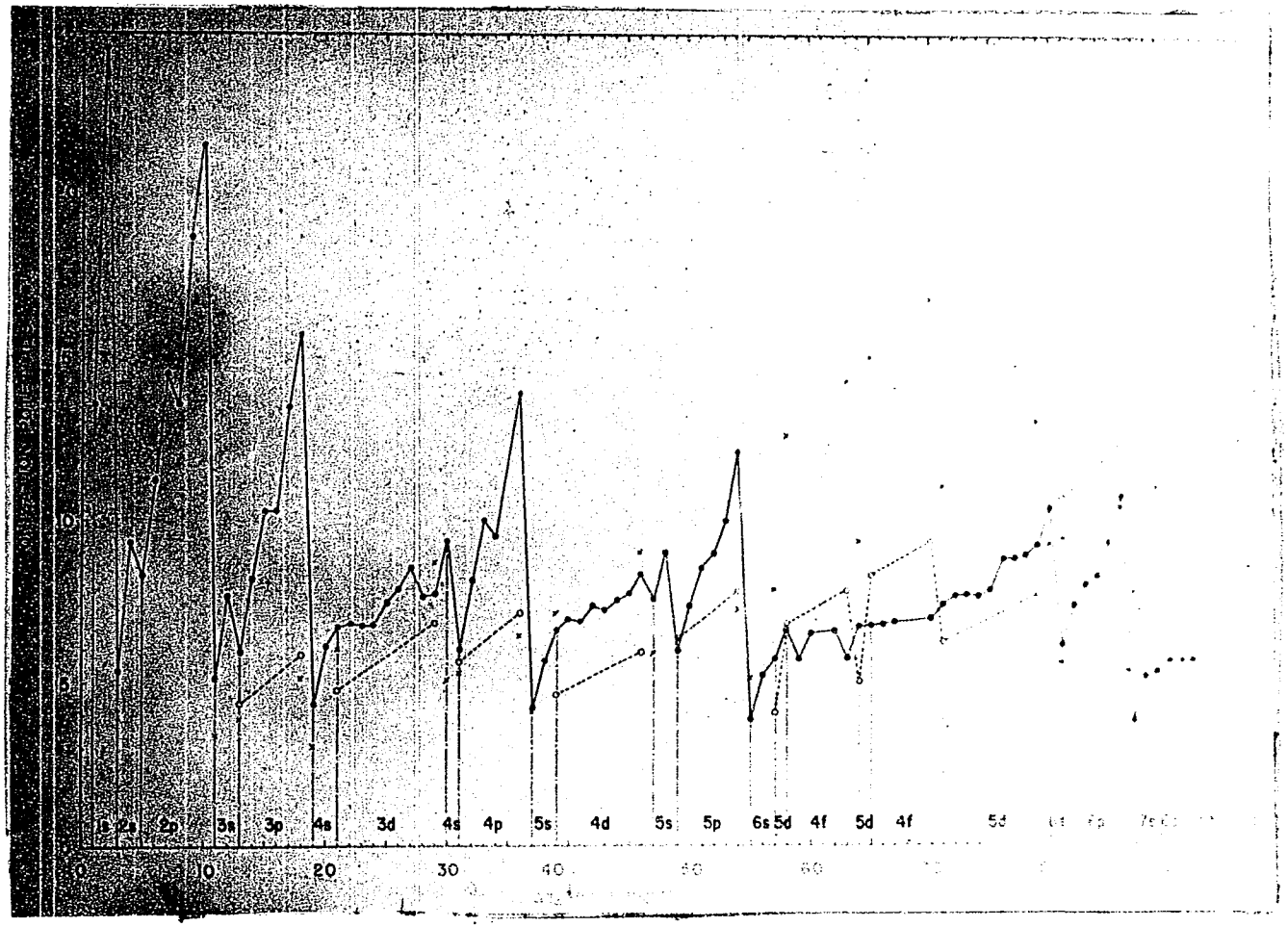

Fig. 7.

Fig. 8. The solution of the Fermi-Thomas equation as found by a differential analyser is indicated as curve 1. Curve 2 is the universal function $\varphi(x)$ that gives the effective nuclear charge as used in this thesis.

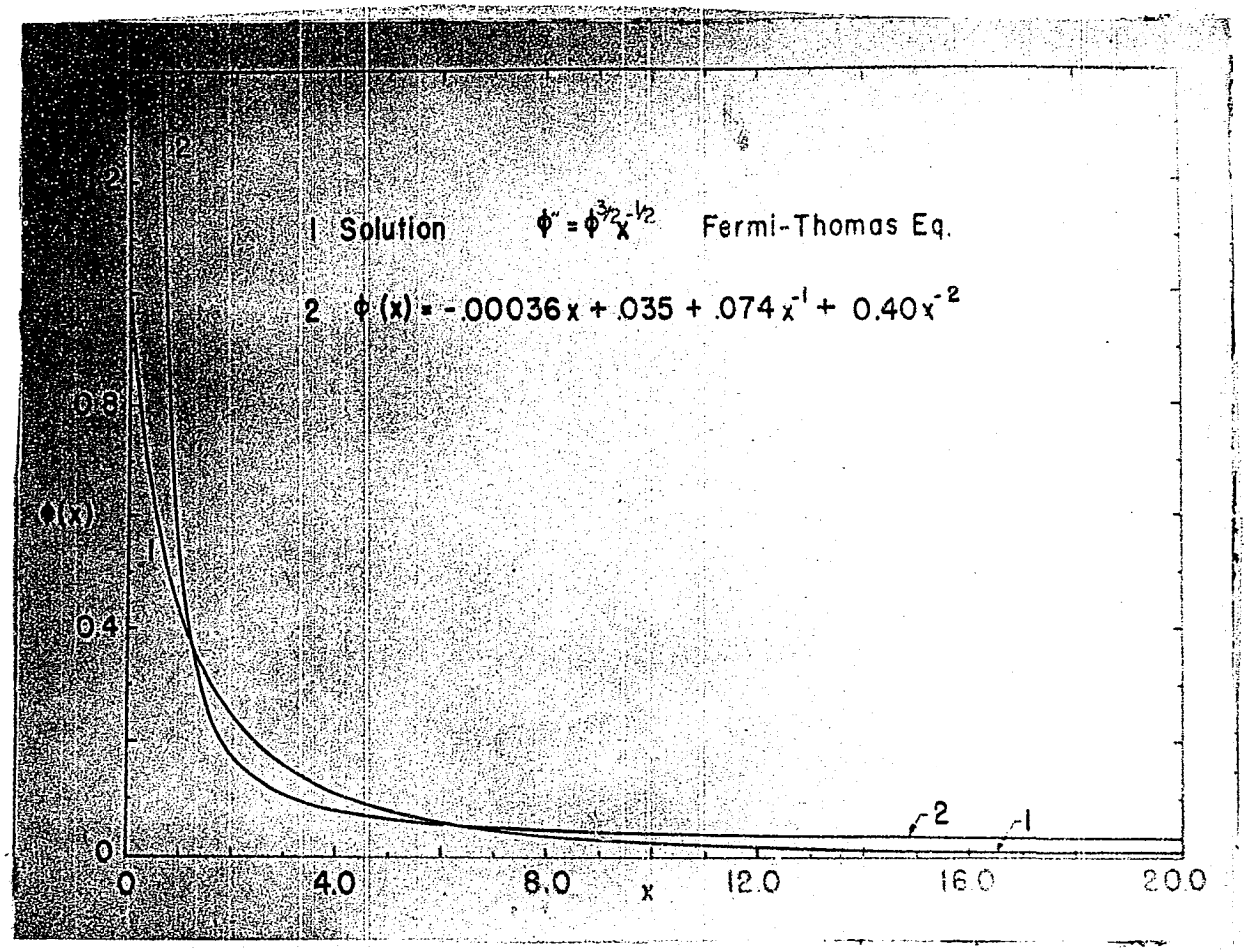

Fig. 8.